Influence of High-Order Twisting Phases on Polarization States and Optical Angular Momentum of a Vector Light Field

Baoyin Liu , Yingqi Huang , Caixia Liu , Shu-Dan Wu , Khian-Hooi Chew , Rui-Pin Chen *

Posted Date: 17 August 2023

doi: 10.20944/preprints202308.1225.v1

Keywords: high-order twisting phases; state of polarization; vector optical fields; orbital angular momentum

Article

Influence of High-Order Twisting Phases on Polarization States and Optical Angular Momentum of a Vector Light Field

Baoyin Liu, Yingqi Huang, Caixia Liu, Shudan Wu, Khian-Hooi Chew and Rui-Pin Chen *

Key Laboratory of Optical Field Manipulation of Zhejiang Province, Department of Physics, Zhejiang Sci-Tech University, Hangzhou, 310018, China; 202020103080@mails.zstu.edu.cn (B.L.); 202120103091@mails.zstu.edu.cn (Y.H.); 202110301010@mails.zstu.edu.cn (C.L.); 202120103109@mails.zstu.edu.cn (S.W.); khchew@um.edu.my (K.-H.C.)

* Correspondence: chenrp@zstu.edu.cn

Abstract: We study the influence of high-order twisting phases on polarization states and optical angular momentum of a vector light field with locally linear polarization and a hybrid state of polarization (SoP). The initial SoP of a twisted vector optical field (TVOF) modulated by the high-order twisting phase possesses various symmetric distributions. The propagating properties of a high-order TVOF with locally linear polarization and hybrid SoP are explored, including the intensity compression, expansion, and conversion between the linear and circular polarization components. In particular, orbital angular momentum (OAM) appears in a high-order TVOF during propagation where no OAM exists in the initial field. The variation of OAM distribution in cross-section becomes more frequent with the increase of the twisting phase order. In addition, a non-symmetric OAM distribution appears in an anisotropic TVOF, leading to the rotation of the beam around the propagation axis during propagation. These results provide a new approach for optical field manipulation in a high-order TVOF.

Keywords: high-order twisting phases; state of polarization; vector optical fields; orbital angular momentum

1. Introduction

In recent years, vector optical fields have attracted significant attention due to their unique properties and wide-ranging applications in various fields, including optical communications [1], imaging [2], and beam manipulation. These vector fields can possess characteristics such as complex spatial structures [3], nonuniform polarization distribution [4,5], and novel phase distributions [6], providing a new way to manipulate light precisely [7]. The concept of phase modulation in vector optical fields originates from the study of wave optics and optical phase engineering. Early investigations focused on controlling the spatial phase distribution [8,9] of light waves, leading to the development of techniques such as spatial light modulators (SLMs) [10] and holography [11,12]. These methods allowed for the precise manipulation of phase profiles, enabling the generation of structured light beams with tailored phase distributions [13]. Building upon these foundational works, researchers began to explore the effect of spatial phase modulation on the scalar beam and the vector optical fields. Many novel properties have been demonstrated with the effect of different phase distributions on a vector optical field [14–18].

In 1993, Simon and Mukunda discovered an inseparable quadratic phase [19], termed the twist phase, while searching for rotationally invariant partially coherent light fields. This twist phase can induce beam rotation during transmission [20]. Research indicated that the twist phase can only exist in partially coherent light fields due to constraints imposed by non-negative-definiteness conditions [21]. In 2019, a new separable twisting phase was proposed [22], introducing the twist phase into fully coherent beams. This provided a new method for generating and measuring scalar vortex beams. In

Preprints (www.preprints.org) | NOT PEER-REVIEWED | Posted: 17 August 2023 doi:10.20944/preprints202308.1225.v1

2021, a high-order twisting phase (cross-phase) was introduced into Bessel-Gaussian beams [23], offering a novel approach to shaping perfect optical vortices. Recently, we introduced the twisting phase into vector beams, revealing that vector vortex beams can be dynamically manipulated using the twisting phase [24]. Nevertheless, to date, the investigation of the effect of high-order twisting phases on a vector light field still needs to be explored.

In this study, we investigated the properties of vector optical fields with high-order twisting phases. The effect of a high-order twisting phase on the initial polarization distribution of vector beams was analyzed. In particular, the evolution of polarization and orbital angular momentum in vector optical fields with high-order twisting phases during propagation is demonstrated. The results also contribute to the deeper understanding and utilization of twisted vector optical fields and shed light on the origin and development of the corresponding research area, such as optical trapping, high-capacity optical communications, and the generation of structured light for advanced imaging and manipulation techniques.

2. Evolution of polarization state in a high-order twisted vector optical field

The form of the general twisting phase δ(x, y) in Cartesian coordinates (x, y) is

$$\delta(x,y) = ux^p y^q \tag{1}$$

where u is the twisted strength of the twisting phase. The exponents p and q are both positive integers. The sum $p+q$ is referred to as the order of the twisted phase. When both exponents are equal to 1 (resulting in a sum of 2), it is termed a low-order twisting phase. Conversely, when the sum is greater than 2 (i.e., $p+q>2$), it is referred to as a high-order twisting phase. The twisted vector optical field at the source plane with a twisting phase can be expressed as follows

$$E(x,y) = \exp(-x^2/\sigma_x^2)\exp\left(-y^2/\sigma_y^2\right)\cdot[\exp(i\delta)\cdot\boldsymbol{e_1} + \exp(-i\delta)\cdot\boldsymbol{e_2}] \tag{2}$$

where σ_x and σ_y is the waist radius of the beam in x- and y- directions, respectively. $\boldsymbol{e_1} = \left(\boldsymbol{e_x} - \exp(\mathrm{i}\Delta\theta)\boldsymbol{e_y}\right), \boldsymbol{e_2} = \left(\boldsymbol{e_x} + \exp(\mathrm{i}\Delta\theta)\boldsymbol{e_y}\right)$. $\boldsymbol{e_x}$ and $\boldsymbol{e_y}$ are the unit vectors in the x- and y-directions, respectively. When $\Delta\theta = 0$, different spatial positions on the cross-section exhibit various states of polarization (SoP), including linear, circular and elliptical polarization. If $\Delta\theta = \pi/2$, different polarization directions of locally linear polarization can be observed at different positions on the initial wavefront. The initial SoP for high-order twisted vector beams with locally linear polarization ($\Delta\theta = \pi/2$) and hybrid polarization ($\Delta\theta = 0$) are depicted in Figure 1, represented by the Stokes parameters S_0 (total intensity), S_1(the linear polarization components in the horizontal and vertical direction), S_2(the linear polarization components of 45°and 135°), and S_3 (the left and right circular polarization components). By comparing the differences of SoP between locally linear polarization (as shown in Figure 1a) and hybrid SoP (as shown in Figure 1b), it can be observed that their S_2 and S_3 parameters are mutually interchangeable, i.e., the S_2 (or S_3) of a high-order twisted vector beam with locally linear polarization is similar to the S_3 (or S_2) of the high-order twisted vector beam with locally linear polarization. The SoP distributions of the initial fields are modulated by the twisting phases, as shown in Figure 1. As recognized from Eq. (1), E (x, y) = $\exp(-x^2/\sigma_x^2)\exp(-y^2/\sigma_y^2)\cdot[\exp(\mathrm{i}\delta)\boldsymbol{e_1} + \exp(-\mathrm{i}\delta)\boldsymbol{e_2}] = \exp(-x^2/\sigma_x^2)\exp(-y^2/\sigma_y^2)\cdot[\cos\delta\cdot\boldsymbol{e_x} + \exp(\mathrm{i}\Delta\theta)\sin\delta\cdot\boldsymbol{e_y}]$. As the position approaches the origin (the values of x and y tend to be zero), the y-direction polarization component goes to zero to form a x- polarized linear polarization. With the increase of the twisting phase orders, the region with x- linear polarization in the beam center becomes broader, as evident from the distribution of S_1 in Figure 1. If $\Delta\theta$=0, when the order of twisting phase p (or q) is odd, it results in a symmetrical amplitude modulation to the SoP about the x-axis but an antisymmetrical amplitude modulation about the y-axis. For $\Delta\theta = \pi/2$, the odd order of twisting phase p (or q) leads to a symmetrical phase modulation to the SoP about the x-axis but an antisymmetrical phase modulation about the y-axis. However, if the order of twisting phase p (or q) is even, the modulations of the high-order twisting phase to the SoP in the initial cross-section are symmetrical about the x (or y) axis either $\Delta\theta$=0 or $\pi/2$, as shown in the first column in Figure 1.

Preprints (www.preprints.org) | NOT PEER-REVIEWED | Posted: 17 August 2023 doi:10.20944/preprints202308.1225.v1

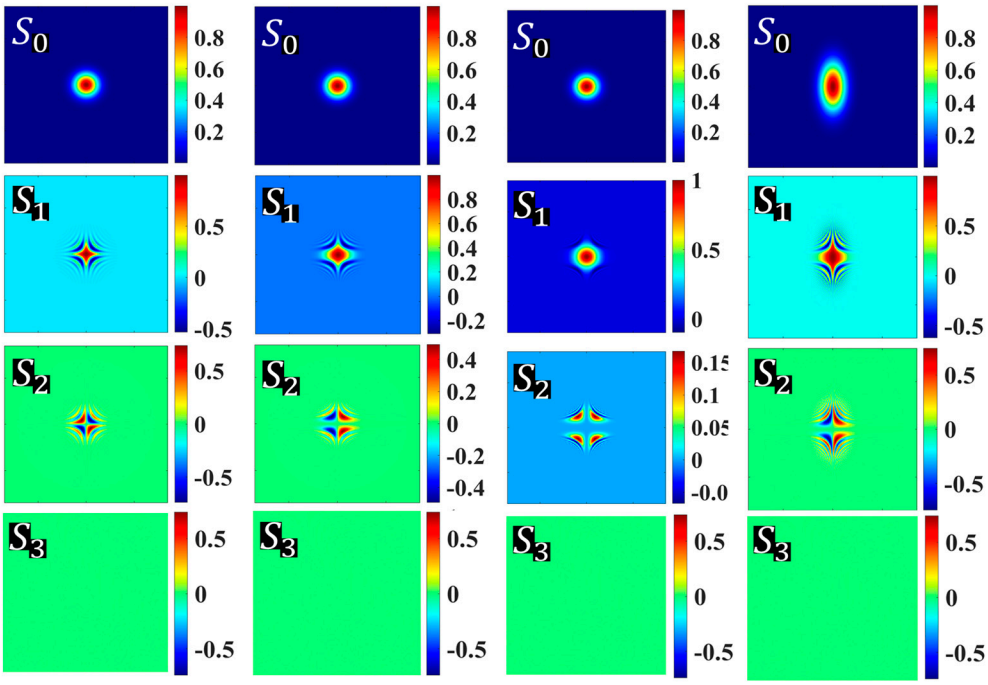

(a)

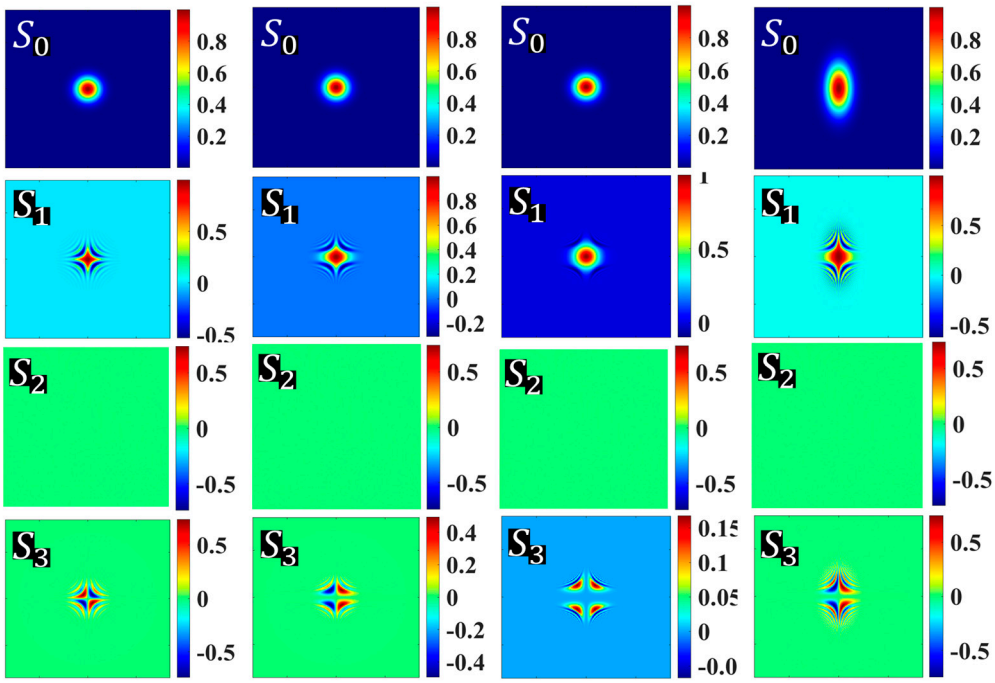

(b)

Figure 1. The Stokes parameters of twisted vector beams under different modulation parameters. The parameters in the figure from columns 1 to 4 are, sequentially: p=1, q=1, u=12×10^6; p=1, q=2, u=12×10^9; p=2, q=4, u=12×10^{18}; p=1, q=2, u=12×10^9. Plots in columns 1-3 represent isotropic beams with $\sigma_x = \sigma_y$ = 0.9mm, while column 4 represents an anisotropic beam with $2\sigma_x = \sigma_y$ = 1.8mm. Here the size of each plot is 8500λ×8500λ. (a) Locally linear polarized light field; (b) hybrid polarized light field.

For the twisted vector optical field with a high-order twisting phase, the distributions of SoP (represented by the Stokes parameters) exhibit the following properties. The distributions of S_0 and

Preprints (www.preprints.org) | NOT PEER-REVIEWED | Posted: 17 August 2023 doi:10.20944/preprints202308.1225.v1

S_1 always appear symmetric about the x or y-axis, denoting the symmetric distributions of total intensity, x or y component intensity, as shown in Figure 1. In the case of locally linear polarized optical fields (see Figure 1(a)), when both p and q are odd, the S_2 distributions show symmetric about the origin but antisymmetric about the x and y-axis, representing the directions of polarization are symmetric about the origin but antisymmetric about x and y axis, as shown in the first column in Figure 1(a) for p=1 and q=1. If p (or q) is odd but q (or p) is even, the S_2 is symmetric about y (or x) axis but antisymmetric about the x (or y) axis. This corresponds to the directions of polarization that are symmetric about the x (or y) axis but antisymmetric about the y (or x) axis, as shown in the second and fourth columns in Figure 1(a) for p=1 and q=2. For the hybrid SoP ($\Delta\theta$=0), the variation of initial SoP distributions with the high-order twisting phase modulations are represented by S_3 (replaced with S_2 for locally linear polarization in Figure 1(a)), as shown in Figure 1(b), denoting the polarization direction changes of circular polarizations resulted from the modulation of high-order twisting phases. It is seen that the fundamental physical properties resulting from the twisted phase are similar to that of the locally linear polarization described above.

Under the paraxial approximation conditions, the vector twisted optical beam propagating in free space can be expressed in the following form using the Rayleigh-Sommerfeld diffraction integral formula,

$$E_x(x,y,z) = -\frac{iz}{\lambda}\frac{e^{ikz}}{z^2}\int_{-\infty}^{\infty}\int_{-\infty}^{\infty} E_{x0}\cdot\exp\left(-\frac{x^2}{\sigma_x^2}\right)\exp\left(-\frac{y^2}{\sigma_y^2}\right)\exp\left(ik\frac{x_0^2+y_0^2-2xx_0-2yy_0}{2z}\right)dx_0\,dy_0,$$
$$E_y(x,y,z) = -\frac{iz}{\lambda}\frac{e^{ikz}}{z^2}\int_{-\infty}^{\infty}\int_{-\infty}^{\infty} E_{y0}\cdot\exp\left(-\frac{x^2}{\sigma_x^2}\right)\exp\left(-\frac{y^2}{\sigma_y^2}\right)\exp\left(ik\frac{x_0^2+y_0^2-2xx_0-2yy_0}{2z}\right)dx_0\,dy_0. \quad (3)$$

Similar to scalar twisted light fields [25,26], the vector light fields carrying a twisting phase experience gradual compression and expansion during propagation in free space. Conversions between linear and circular polarizations in a twisted vector light field occur during propagation. When the initial light field is locally linearly polarized, the conversion to circular polarization from linear polarization during propagation leads to S_3 no longer being entirely zero as shown in Figure 2(a). The 45° and 135° linear polarization components appear for the hybrid polarized twisted vector beam as the variation of S_2 values in Figure 2(b). All polarization components and the whole field perform gradual compression and expansion during propagation. For the anisotropic beams with $\sigma_x \neq \sigma_y$ [22,23], the influence of the high-order twisting phase on the SoP is similar to that of isotropic beams with $\sigma_x=\sigma_y$. However, the intensity distribution of anisotropic beams is elliptical, unlike the circular shape of isotropic beams. Moreover, the anisotropic twisted vector beam experience rotation during propagation, as depicted in Figure 2(c).

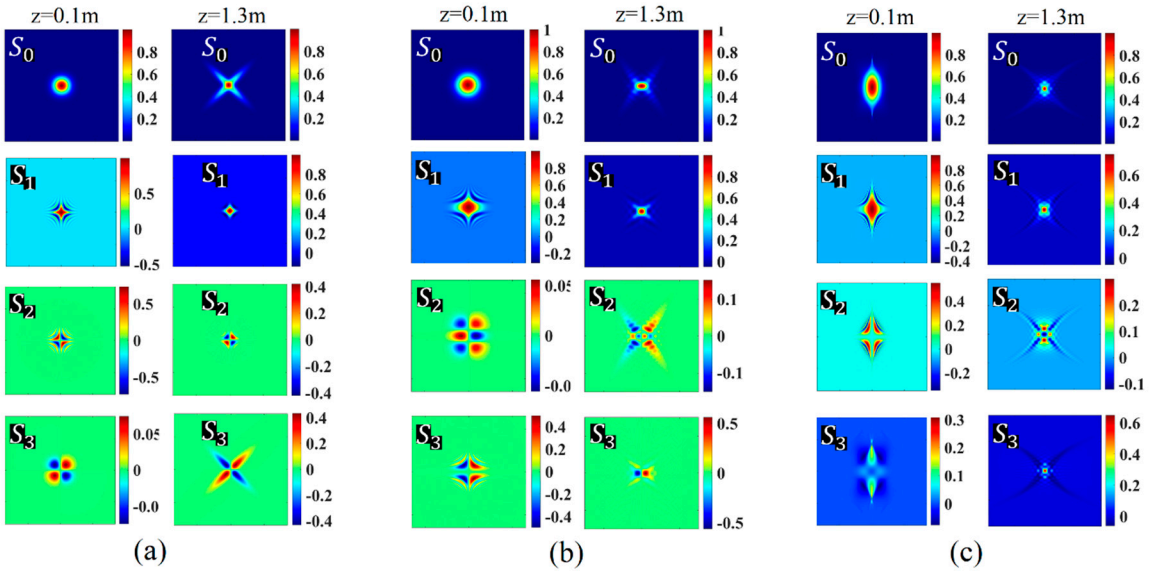

Preprints (www.preprints.org) | NOT PEER-REVIEWED | Posted: 17 August 2023 doi:10.20944/preprints202308.1225.v1

Figure 2. The Stokes parameters of various TVOF during transmission: (a) isotropic (σ_x=σ_y=0.9mm) locally linearly polarized twisted vector optical beam, p=1, q=1, u=12×10^6; (b) isotropic (σ_x=σ_y=0.9mm) hybrid-polarized twisted vector optical beam, p=1, q=2, u=12×10^9; (c) anisotropic (2σ_x=σ_y=1.8mm) locally linearly polarized twisted vector optical beam, p=2, q=2, u=12×10^{12}.

3. Effect of a high-order twisting phase on the optical angular momentum

Polarization conversions between linear and circular, and the manipulation of optical angular momentum in structured light fields are important topics in optical field manipulation, with significant fundamental research interest and practical applications. The spin angular momentum (SAM) relies on circular polarization (referred to the S_3 in Figure 2), while the OAM is related to the gradient phase distribution [27]. The SAM and OAM densities of structured beams in the focal region can be calculated as follows:

$$S \propto \mathrm{Im}[E *\times E]$$
$$L \propto \mathrm{Im}[r \times (E *\cdot (\nabla)E)] \quad (4)$$

where Im[.] denotes the imaginary part, and the asterisk represents complex conjugation. S and L describe the SAM and OAM densities, respectively. The linear-circular polarization conversion during propagation leads to the SAM appearance even if there is no SAM in the initial field for the locally linear twisted vector optical field, represented by S_3 as shown in Figure 2(a). The evolutions of SAM in a twisted vector optical field (TVOF) and conversions between linear and circular polarizations for both locally linear polarized and hybrid SoP during propagation are sensitively dependent to the twisting phase orders p and q as shown in Figure 2.

Distinct from the spin angular momentum associated with circular polarization, the OAM characteristics are related to the gradient phase distribution. There are no OAM distributions in the initial TVOF. However, different (positive and negative) OAM distributions in the cross-section will appear because of the twisting phase during propagation, as shown in Figure 3. The effect of a low-order twisting phase is similar to that of cylindrical lenses [28], leading to the generation of OAM [29]. With the increase of the twisting phase order, the variation of OAM distribution becomes more frequent, leading to more (positive or negative) extreme values of OAM distribution in the cross-section. In particular, a nonsymmetric OAM distribution appears due to the unequal field distributions in x and y directions for an anisotropic TVOF, leading to the beam rotation during propagation, as shown in Figure 3(c) for 2σ_x=σ_y=1.8mm. These results offer a new approach to manipulate the SoP and optical angular momentum in a high-order TVOF.

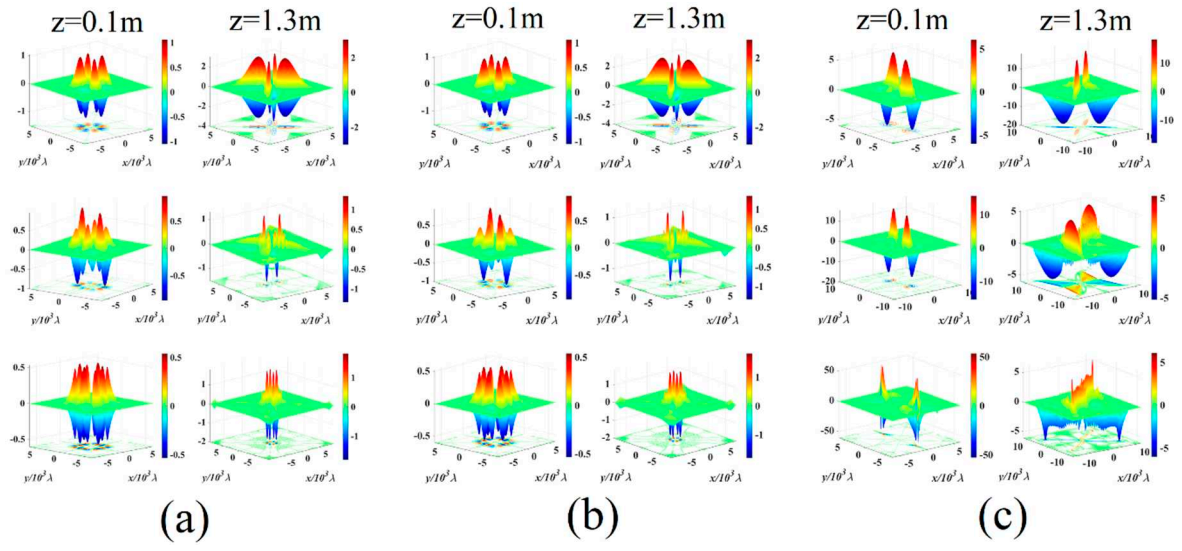

Figure 3. The OAM evolution of TVOF under different parameters: (a) isotropic (σ_x=σ_y=0.9mm), locally linearly polarized; (b) isotropic (σ_x=σ_y=0.9mm), hybrid-polarized; (c) anisotropic (2σ_x = σ_y =

1.8mm), locally linearly polarized. The first, second and third rows are sequentially: p=1, q = 1; p =1, q = 2 and p =2, q = 2.

4. Discussion

As a novel phase, the effect of a high-order twisting phase on TVOF with locally linear polarization and a hybrid SoP results in novel SoP distributions and propagation dynamics. Similar to the low-order twisting phase with p=1 and q=1, the TVOF with high-order twisting phases also performs the intensity compression and expansion, conversion between the linear and circular polarizations and the appearance of OAM during propagation. However, with the order increase of the high-order twisting phase, these phenomena occur earlier and the variation of OAM distribution becomes more frequent during propagation. Nonsymmetric OAM distributions appear in anisotropic TVOF ($\sigma_x \neq \sigma_y$) which are closely related to the orders of twisting phases, leading to the rotation of the beam around the propagation axis. The findings presented in this study offer valuable insights into the properties and behavior of vector optical fields with high-order twisting phase modulation, providing a foundation for further advancements in optical field manipulation and potential applications in optical communications, imaging, and micro-particle manipulation.

5. Conclusion

In summary, the influence of the high-order twisting phase on polarization states and the optical angular momentum of a vector light field is investigated in this work. The initial SoP of a TVOF is modulated by the high-order twisting phases, leading to novel SoP distributions with various symmetries. The propagating properties of high-order TVOF with locally linear polarization and hybrid SoP are explored including the intensity compression and expansion, conversion between the linear and circular polarization components, and appearance of OAM during propagation. These phenomena occur earlier with the increasing order of the twisting phase. In addition, a nonsymmetric OAM distribution appears in an anisotropic TVOF, leading to beam rotation around the propagation axis during propagation. These findings offer a new approach to optical field manipulation and may find potential applications in the corresponding field.

Author Contributions: Conceptualization, R.-P.C.; methodology, R.-P.C. and B.L.; validation, R.-P.C. and K.-H.C.; investigation, B.L., C.L., Y.H. and R.-P.C.; data curation, B.L., C.L., Y.H., S.W., and R.-P.C.; supervision, R.-P.C.; writing—original draft preparation, B.L.; writing—review and editing, R.-P.C. and K.-H.C. All authors have read and agreed to the published version of the manuscript.

Funding: This research was funded by the Zhejiang Provincial Key Research and Development Program (No. 2022C04007); National Natural Science Foundation of China (No. 11874323).

Institutional Review Board Statement: Not applicable.

Informed Consent Statement: Not applicable.

Data Availability Statement: Not applicable.

Conflicts of Interest: The authors declare no conflict of interest.

References

1. Ndagano, B.; Nape, I.; Cox, M.A.; Rosales-Guzman, C.; Forbes, A. Creation and detection of vector vortex modes for classical and quantum communication. *J. Light. Technol.* **2018**, *36*, 292–301, doi:10.1109/JLT.2017.2766760.
2. O'Holleran, K.; Flossmann, F.; Dennis, M.R.; Padgett, M.J. Methodology for imaging the 3D structure of singularities in scalar and vector optical fields. *J. Opt. Pure Appl. Opt.* **2009**, *11*, 094020, doi:10.1088/1464-4258/11/9/094020.
3. Yao, G.; Li, Y.; Chen, R.-P. Collapse dynamics of vortex beams in a Kerr medium with refractive index modulation and PT-symmetric lattices. *Photonics* **2022**, *9*, 249, doi:10.3390/photonics9040249.
4. Liu, C.; Li, Y.; Wu, F.; Chen, R.-P. Polarization state evolution of a twisted vector optical field in a strongly nonlocal nonlinear medium. *J. Opt. Soc. Am. A* **2023**, *40*, 620, doi:10.1364/JOSAA.484221.

5. Zhou, Y.; Lin, X.; Liao, M.; Zhao, G.; Fang, Y. Polarization manipulation of bright-dark vector bisolitons. *Chin. Phys. B* **2021**, *30*, 034208, doi:10.1088/1674-1056/abd76d.
6. Buryy, O.; Andrushchak, A.; Chernovol, N. The optimal geometries of phase matching in uniaxial nonlinear optical crystals determined by extreme surfaces method. In Proceedings of the 2020 IEEE 15th International Conference on Advanced Trends in Radioelectronics, Telecommunications and Computer Engineering (TCSET); IEEE: Lviv-Slavske, Ukraine, February 2020; pp. 436–441.
7. Hu, X.-B.; Zhao, B.; Chen, R.-P.; Rosales-Guzmán, C. Experimental generation of arbitrary abruptly autofusing circular Airy Gaussian vortex vector beams. *Sci. Rep.* **2022**, *12*, 18274, doi:10.1038/s41598-022-23157-1.
8. Toussaint, K.C.; Park, S.; Jureller, J.E.; Scherer, N.F. Generation of optical vector beams with a diffractive optical element interferometer. *Opt. Lett.* **2005**, *30*, 2846, doi:10.1364/OL.30.002846.
9. De Oliveira, A.G.; Rubiano Da Silva, N.; Medeiros De Araújo, R.; Souto Ribeiro, P.H.; Walborn, S.P. Quantum optical description of phase conjugation of vector vortex beams in stimulated parametric down-conversion. *Phys. Rev. Appl.* **2020**, *14*, 024048, doi:10.1103/PhysRevApplied.14.024048.
10. Beversluis, M.R.; Novotny, L.; Stranick, S.J. Programmable vector point-spread function engineering. *Opt. Express* **2006**, *14*, 2650, doi:10.1364/OE.14.002650.
11. Bomzon, Z.; Kleiner, V.; Hasman, E. Formation of radially and azimuthally polarized light using space-variant subwavelength metal stripe gratings. *Appl. Phys. Lett.* **2001**, *79*, 1587–1589, doi:10.1063/1.1401091.
12. Niv, A.; Biener, G.; Kleiner, V.; Hasman, E. Propagation-invariant vectorial Bessel beams obtained by use of quantized Pancharatnam–Berry phase optical elements. *Opt. Lett.* **2004**, *29*, 238, doi:10.1364/OL.29.000238.
13. Chen, H.; Hao, J.; Zhang, B.-F.; Xu, J.; Ding, J.; Wang, H.-T. Generation of vector beam with space-variant distribution of both polarization and phase. *Opt. Lett.* **2011**, *36*, 3179, doi:10.1364/OL.36.003179.
14. Zhang, X.; Chew, K.-H.; Liu, C.; Wang, Z.; Chen, R.-P. Controllable linear-circular polarization conversion of radial variant vector beams in a strongly nonlocal nonlinear medium. *J. Opt.* **2019**, *21*, 065402, doi:10.1088/2040-8986/ab202d.
15. Yue, Z.; Lu, P.; Xu, J.; Li, Z.; Teng, S. Vector beams encoded by diverse orthogonal polarization states and their generation based on metasurfaces. *New J. Phys.* **2023**, *25*, 013018, doi:10.1088/1367-2630/aca787.
16. Li, M.; Yue, X.; Xu, T. Asymptotic behaviors of mixed-type vector double-pole solutions for the discrete coupled nonlinear Schrödinger system. *Eur. Phys. J. Plus* **2021**, *136*, 62, doi:10.1140/epjp/s13360-020-01040-0.
17. Spall, J.; Guo, X.; Barrett, T.D.; Lvovsky, A.I. Fully reconfigurable coherent optical vector–matrix multiplication. *Opt. Lett.* **2020**, *45*, 5752, doi:10.1364/OL.401675.
18. Long, Z.; Hu, H.; Ma, X.; Tai, Y.; Li, X. Encoding and decoding communications based on perfect vector optical vortex arrays. *J. Phys. Appl. Phys.* **2022**, *55*, 435105, doi:10.1088/1361-6463/ac8d13.
19. Simon, R.; Mukunda, N. Twisted Gaussian Schell-model beams. *J. Opt. Soc. Am. A* **1993**, *10*, 95, doi:10.1364/JOSAA.10.000095.
20. Friberg, A.T.; Tervonen, E.; Turunen, J. Focusing of twisted Gaussian Schell-model beams. *Opt. Commun.* **1994**, *106*, 127–132, doi:10.1016/0030-4018(94)90308-5.
21. 21. Wan, L.; Zhao, D. Generalized partially coherent beams with nonseparable phases. *Opt. Lett.* **2019**, *44*, 4714, doi:10.1364/OL.44.004714.
22. Liang, G.; Wang, Q. Controllable conversion between Hermite Gaussian and Laguerre Gaussian modes due to cross phase. *Opt. Express* **2019**, *27*, 10684, doi:10.1364/OE.27.010684.
23. Wang, C.; Ren, Y.; Liu, T.; Liu, Z.; Qiu, S.; Li, Z.; Ding, Y.; Wu, H. Generating a new type of polygonal perfect optical vortex. *Opt. Express* **2021**, *29*, 14126, doi:10.1364/OE.425134.
24. Liu, Q.; Chew, K.-H.; Huang, Y.; Liu, C.; Hu, X.; Li, Y.; Chen, R.-P. Effect of twisting phases on the polarization dynamics of a vector optical field. *Photonics* **2022**, *9*, 722, doi:10.3390/photonics9100722.
25. Desyatnikov, A.S.; Buccoliero, D.; Dennis, M.R.; Kivshar, Y.S. Suppression of collapse for spiraling elliptic solitons. *Phys. Rev. Lett.* **2010**, *104*, 053902, doi:10.1103/PhysRevLett.104.053902.
26. Liang, G.; Guo, Q. Spiraling elliptic solitons in nonlocal nonlinear media without anisotropy. *Phys. Rev. A* **2013**, *88*, 043825, doi:10.1103/PhysRevA.88.043825.
27. Allen, L.; Beijersbergen, M.W.; Spreeuw, R.J.C.; Woerdman, J.P. Orbital angular momentum of light and the transformation of Laguerre-Gaussian laser modes. *Phys. Rev. A* **1992**, *45*, 8185–8189, doi:10.1103/PhysRevA.45.8185.

28. Courtial, J.; Dholakia, K.; Allen, L.; Padgett, M.J. Gaussian beams with very high orbital angular momentum. *Opt. Commun.* **1997**, *144*, 210–213, doi:10.1016/S0030-4018(97)00376-3.
29. Wu, S.-D.; Chew, K.-H.; Chen, R.-P. Effect of twisting phases on linear–circular polarization and spin–orbital angular momentum conversions in tightly focused vector and scalar beams. *Photonics* **2023**, *10*, 151, doi:10.3390/photonics10020151.